2017

Mass Transfer Effects of Particle Size on Brewing Espresso

Sichen Zhong
zhongs@rose-hulman.edu

Lauren Elizabeth Stork
Storkle@rose-hulman.edu

Mass Transfer Effects of Particle Size on Brewing Espresso

Participants: Lauren Stork, Sichen Zhong

Advisor: David Henthorn

Rose-Hulman Institute of Technology Chemical Engineering Department

Dec 12th, 2017

Abstract

The extraction process for coffee is complicated due to the nature of the coffee. In this paper, we studied the particle size distribution for coffee grinds and further analyzed that with the help of an inverted microscope and a scanning electron microscope. We drew a conclusion that the coffee grinds can be divided into two parts: cell fragments with smaller particles size and intact coffee cells with larger particles. The intact coffee cell was found to be a porous media. Therefore, we tried to brew the espresso with both normal grind size coffee and sieved coffee to study the extraction of the coffee as a function of the mass ratio of espresso collected. The high-performance liquid chromatography and mass spectrometry were performed to both espresso prepared by normal grind size coffee and sieved coffee mixed with glass beads. The results showed that the compounds extracted for both brews are mostly identical. We also tried to fit our data to a double porosity mathematical model that was recently published, and we found that the model is not perfect for our espresso brewing conditions.

Introduction

People have been making coffee for centuries, and it has become one of the most widely consumed beverages in the world. [1] The nature of coffee brewing is solid-liquid extraction, which involves the transfer of solutes from a solid to the liquid. Despite its wide consumption, little is known about its production process. While there are many different techniques for brewing coffee, this paper focuses on espresso. Espresso is a concentrated form of coffee that is made by forcing pressurized water, normally at 9 bar and 90-97℃, through a packed bed of finely ground coffee. Recently, researchers have started to develop theories attempting to model the mass transfer of coffee. These theories have led to the creation of espresso power curves, which show the percent of coffee solids extracted from the beans as a function of brewed coffee collected. The y axis of the curve shows the percent of coffee extracted from the coffee grounds, and the x axis shows the mass of coffee collected. The extraction percent was defined as the amount of solids extracted divided by the total mass of coffee put in the coffee bed. While the samples were not evaluated for the taste during this research, expert tasters show a preference for certain extractions and strength. These preferences, as outlined by the Specialty Coffee Association of America (SCAA), are for an extraction percent between 18 and 22 percent and a TDS value of 9 to 13 percent. [2] Figure 1 shows how different strengths and extraction percents change the flavor of the coffee. Power curves can also be used to help better understand the mass transfer rates of coffee because the mass flow rate of water for most commercial grade espresso machines is relatively constant. It can be assumed that these plots show the mass released from the coffee beans as a function of time, because of this relatively constant mass flow rate.
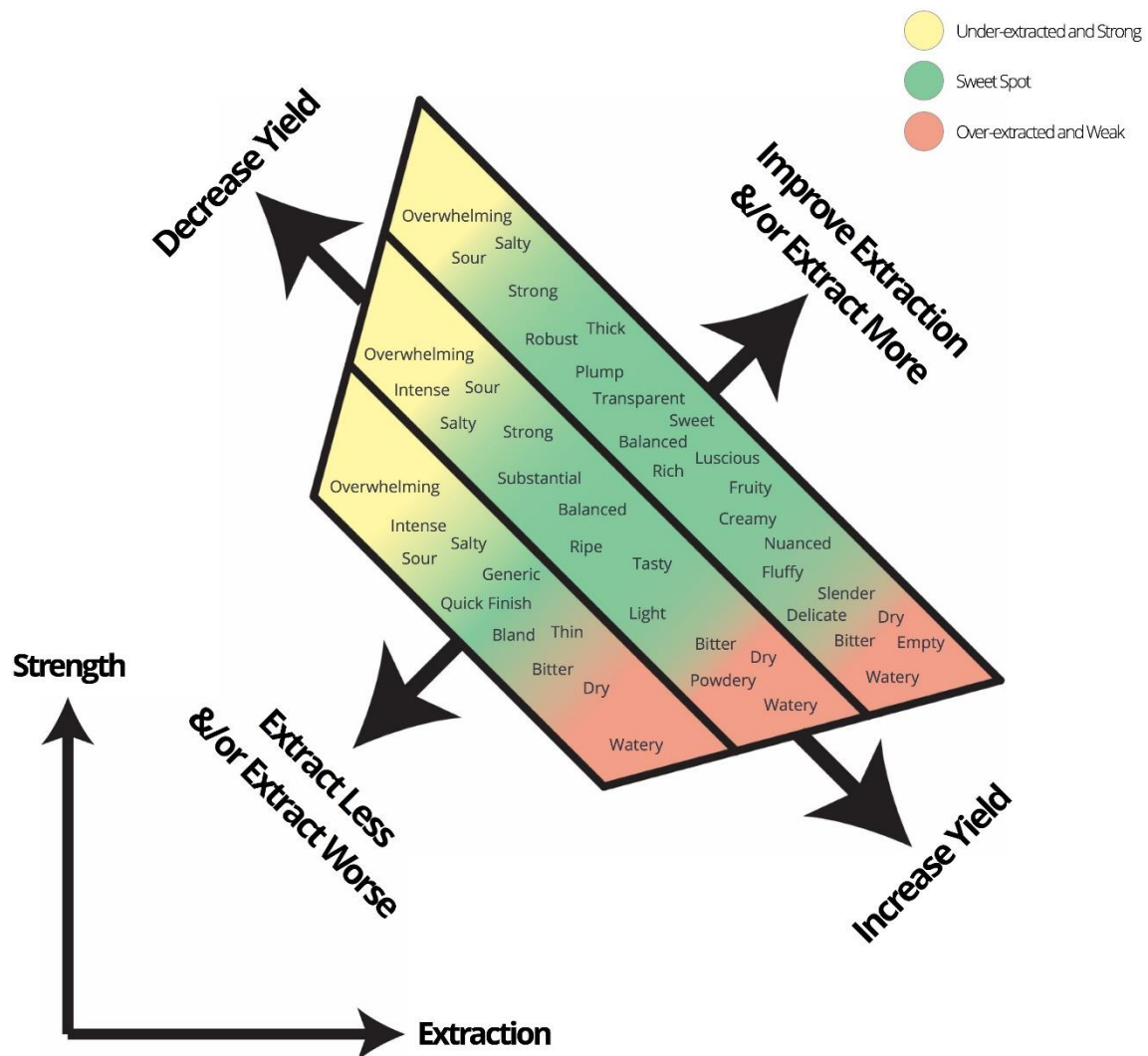
Figure 1 Correlation of Strength and Extraction to perceived taste characteristics [3]

Experimental methods

The coffee used for the following experiments was a Ethiopia Yirgacheffe Aricha roasted on June 13th from Red Bird Coffee, Bozeman, MT. The coffee was ground by Lelit PL53 (Espresso only grinder). The coffee was brewed by Rancilio Silvia V1 Espresso machine with a PID capable of controlling temperature within 1°C. Reverse osmosis purified water with 4 ppm dissolved solids was used.

To better study the mass transfer mechanism of the espresso, we decided to investigate the effect of particle size. Particle size contributes to the control of dissolution rate, because the different sizes will have different surface area. [4] For our experiment,

particle size distribution were determined by using Hydro 2000MU wet sample dispersion unit with the Mastersizer 2000 instrument from Malvern Instrument was used to investigate the particle size distribution for coffee grinds. Dry ground coffee was added to a beaker of deionized water until the laser obscuration was deemed to be in range. Due to the assumption that the rapid extraction observed is explained by the small coffee cell fragments, we decided to focus specifically on the extraction of the fragments. In order to accomplish this, the grind size on the grinder was turned down, and the resulting grains were then put through a 250 µm sieve. Since roasted coffee beans still contain lipids, the coffee grains show the cohesive characteristics. The aggregation of particles makes it hard to pass through the smaller size sieve with sieve shaker. A 250 µm sieve, which has smaller sieve diameter than mean diameter for intact coffee cells, was chosen to reduce the particle size for coffee grains. After sieving the grains, most intact cells were removed. The particle size of sieved coffee was measured using the same instrument as well. To better understand the distribution of particle size, the Olympus CKX41 inverted microscope has been used to take pictures for ground coffee particles. In order to understand the nature of the coffee grounds, a Hitachi S-3000N scanning electron microscope was utilized to study the structure of the coffee particles.

In the experiment, three different masses of coffee grains, 14.5 grams, 16.5 grams, and 18.5 grams, were used to prepare a coffee bed in a VST basket. The PID was set to 101 ℃, and by the time the water went to the coffee bed, it was at a range of 90-95 ℃. Through the experiment, different masses of brewed espresso were collected and a pocket refractometer by ATAGO was used to measure the total dissolved solids. This is used to calculate the extraction yield for brewed coffee. The extraction yield is defined as the mass of dissolved solids in the espresso divided by the mass of ground coffee. The time for brewing coffee was recorded to represent the correlation between extraction yield and time. However, the lag of espresso machine results in a relatively inaccurate time measurement. We assumed

that the mass flow rate of water through the coffee bed is constant. Therefore, the mass of espresso collected is also a time-dependent variable. To better compare the correlation of extraction yield between different mass of coffee used in the experiment, a mass ratio of espresso collected to the mass of coffee put in the basket were used for nondimensionalization.

In order to simulate the circumstance of a typical coffee bed, the 350-400 µm glass beads were mixed with the sieved coffee grains. A mixture of 8 grams of glass beads and 10 grams of coffee grains was used for the experiments to determine the total dissolved solids, and the extraction percent. The mass was converted to a mass ratio in order to be compared to the previous trails.

Liquid Chromatography and Mass Spectroscopy or LC/MS was run on both the normal grind coffee and the coffee brewed from the sieved coffee grains. Both samples were collected at a mass ratio of 2.0. The coffee pushed through a syringe filter with a pore size of 0.22 µm in order to remove undissolved solids, before it was diluted in deionized water. Separation was achieved on an Aqua C18 125 Å, LC Column (250 x 4.6 mm 5 µm) from Phenomenex. The mobile phase for HPLC analysis was water (A) containing 0.1% formic acid and methanol (B), at a flow rate of 0.4 mL/min in 50/50 ratio. The injection volume was 10 µL. HPLC analysis was performed using a Shimadzu LCMS-2020. The PDA was collected at a wavelength of 265 nm.

Mathematical Model

This section attempts to explain a recently developed mathematical model that attempts to simulate the mass transfer of coffee through a system of partial differential equations. A key feature of the model is that the coffee bed is represented by a porous medium domain using a double porosity model. [5] The paper simulates the coffee extraction from a flow through a cylinder similar to the espresso machine, but with lower pressure. [5] The Figure 2 shows a definition for different phases in the coffee bed. There are a series of assumptions listed to better simulate the mass transfer of coffee in the model. Refer to Appendix A, for a list of all the assumptions used from Moroney et al. [5] The system of partial differential equations was coded in Maple and then solved numerically. The code is listed in Appendix B. Due to the difficulty of estimating some constant values, we made the assumption that some constants were kept the same as the Moroney et al. [5] paper values, but several constants were then changed to better fit the method for brewing espresso. The results were then compared to our experimental results in order to determine if and where changes would need to be made to the model.
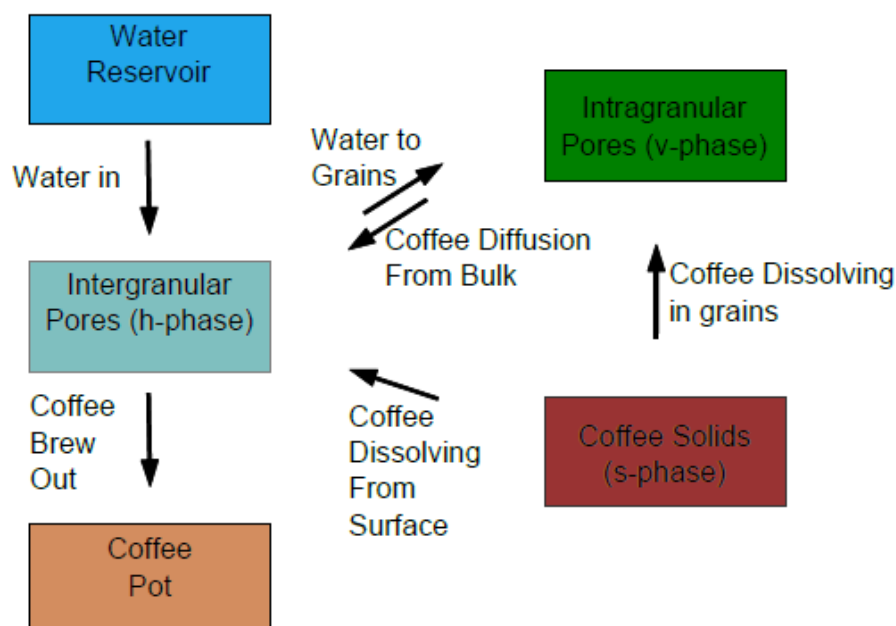

Figure 2 The transfer of water and coffee in different phase [5]

Most of the constants that were presented in the paper were assumed to also be true for our coffee. Constants that were changed to better fit our data were ΔP (the pressure drop across the bed), k_{sv1} (Sauter Mean Diameter of all grains), k_{sv2} (Sauter Mean Diameter of grains greater than 50μm), l_l (mean volume weighted grain radius) m (the coffee cell diameter), and L (the coffee bed height). Table 1 lists all constants used.

Table 1. Parameters for coffee grains from our experiments and for coffee grains from Moroney et al. [5]

Parameter	Description	Our Values	Moroney et al[5]
ϕ_v^∞	intragranular porosity	0.7034	0.7034
ϕ_h	intergranular porosity	0.2	0.2
c_s	coffee solid density	1400 kg m^{-3}	1400 kg m^{-3}
ϕ_{cd}	soluble coffee volume fraction	0.143435	0.143435
$\phi_{s,sd}$	surface coffee volume fraction	0.11	0.11
$\phi_{s,bd}$	grain kernel coffee volume fraction	0.033435	0.033435
α^*	grain diffusion fitting coefficient	0.1833	0.1833
β^*	surface dissolution fitting coefficient	0.0447	0.0447
ΔP	pressure drop across bed	900000 Pa	230000 Pa
L	coffee bed height	0.011 m	0.0405 m
k_{sv1}	Sauter mean diameter (all grains)	56.327 μm	27.35 μm
k_{sv2}	Sauter mean diameter (grains > 50μm)	90.506 μm	322.49 μm
l_l	mean volume weighted grain radius	253.557 μm	282 μm
$D_h = D_v$	coffee diffusion coefficient(for caffeine)	2.2 ·10^{-9} m^{2}s^{-1}	2.2 ·10^{-9} m^{2}s^{-1}
ρ	liquid density (for water at 90˚C)	965.3 kg m^{-3}	965.3 kg m^{-3}
μ	liquid viscosity (for water at 90˚C)	0.315·10^{-3} Pa s	0.315·10^{-3} Pa s
m	coffee cell diameter	176 μm	30 μm
c_{sat}	coffee solubility	212.4 kg m^{-3}	212.4 kg m^{-3}
κ	Kozeny-Carmen shape coefficient	3.1	3.1
η	initial intergranular concentration level	0.5	0.5
Ψ_{s0}^*	fraction of $\phi_{s,sd}$ remaining after filling	0.7304	0.7304
g	acceleration due to gravity	9.8 m s^{-2}	9.8 m s^{-2}

These parameters were used to calculate different timescales. The bulk diffusion timescale, t_d, is the timescale for coffee diffusion from the intergranular pores. The surface dissolution timescale, t_s, is the timescale for which coffee dissolves into the intergranular pores from the grain surfaces. Lastly, the advection timescale, t_a, is the timescale for which

the dissolved coffee is carried out of the bed. [5] These timescales are represented by the following equations.

$$t_d = \frac{k_{sv2} l_l}{6\alpha^* \phi_v^{\infty \frac{1}{3}} D_v}$$ (1)

$$t_s = \frac{k_{sv1} m \phi_h}{12\beta^* D_h \phi_{cd} \psi_{s0}^* (1 - \phi_h)}$$ (2)

$$t_a = \frac{36 L^2 \kappa \mu (1 - \phi_h)^2}{k_{sv1}^2 \phi_h^2 (\Delta P + \rho g L)}$$ (3)

Next in order to make the equations tidier, several non-dimensional parameters were defined. The parameter ε is defined as the ratio between the advection timescale and the diffusion timescale. [5] This is demonstrated by

$$\epsilon = \frac{216 \kappa \mu L^2 \alpha^* D_v \phi_v^{\infty \frac{1}{3}} (1 - \phi_h)^2}{k_{sv2} k_{sv1}^2 \phi_h^2 l_l (\Delta P + \rho g L)} = \frac{t_a}{t_d}$$ (4)

The other three non-dimensional numbers are,

$$a_1 = \frac{1 - \phi_h}{\phi_h} \phi_v^{\infty}$$ (5)

$$a_2 = \frac{432 \kappa \mu L^2 \beta^* D_h \phi_{cd} \psi_{s0}^* (1 - \phi_h)^3}{k_{sv1}^3 m \phi_h^3 (\Delta P + \rho g L)} = \frac{t_a}{t_s}$$ (6)

$$a_3 = \frac{c_{sat} r_s \phi_h}{c_s (1 - \phi_h) \psi_{s0}^*}$$ (7)

These non-dimensional numbers are used in the partial differential equations. When using the parameters from Moroney et al [5] paper these numbers have values of, $\epsilon = 0.127$, $a_1 = 2.81$, $a_2 = 3.23$, $a_3 = 0.473$. When using the parameters from the espresso experiments these numbers have values of, $\epsilon = 0.002235$, $a_1 = 2.81$, $a_2 = 0.001189$, $a_3 = 0.473$. All the values above are calculated based on the constant values from Table 1.

In terms of the non-dimensionalized numbers the proposed system of partial differential equations are as follows. Equation 8 represents the solution to C_h, where C_h is the concentration of coffee in the h phase. H phase refers to the intergranular phase or the space between grains of coffee. Equation 9 represents the solution to C_v, where C_v is the concentration of coffee in the v phase. V phase refers to the intragranular phase, or the porous space inside the grains. Lastly, equation 10 represents the solution to Ψ_s, where Ψ_s is a nondimensionalized fraction of coffee remaining in the s phase. The s phase is the coffee solid phase and should dissolve away during the coffee extraction process. The main assumption here is that while the s phase has coffee on the surface of the particles and in the porous kernels, only the surface contributes to the extraction due to the short duration of the espresso.

$$\epsilon \frac{\partial C_h}{\partial \tau} = \frac{\partial C_h}{\partial z} - \epsilon a_1 C_h + C_v + (1 - a_1 \epsilon C_h)\Psi_s \tag{8}$$

$$\frac{\partial C_v}{\partial \tau} = a_1 \epsilon C_h - C_v \tag{9}$$

$$\epsilon \frac{\partial \Psi_s}{\partial \tau} = -a_2 a_3 (1 - a_1 \epsilon C_h)\Psi_s \tag{10}$$

This system of equations is solved using the following set of initial and boundary conditions.

$$0 < z < 1 \tag{11}$$

$$\tau > 0 \tag{12}$$

$$C_h(z, 0) = \frac{1}{a_1 \epsilon} \tag{13}$$

$$C_v(z, 0) = \eta \tag{14}$$

$$\Psi_s(z, 0) = \frac{a_2 \psi_{s0}^*}{a_1 \epsilon} \tag{15}$$

$$C_h(1, \tau) = 0 \tag{16}$$

The perturbation method was used to determine the approximation solutions to different timescales. In summary, the inner and outer solutions were approximated for different phases. According to paper from Moroney et al [5], for C_h we obtain an expansion

to leading order in the inner layer and to O(ϵ) in the outer region. The solution for C_v is known to O(ϵ) in both regions, while ψ_s has an inner solution at leading order while the outer solution is 0 to O(ϵ). The approximated equations were incorporated with Heaviside functions to involve different mechanisms. The equations used to approximate are as follows,

$$c_h(z,t) = \left(1 + \epsilon\left(\frac{a_1 e^{-a_2 t}(\eta-1)(e^{a_2 t}-1)}{a_2}\right)\right)H(1-(z+t))$$
$$+ \left(\frac{e^{a_2}-e^{a_2 z}}{e^{a_2}-e^{a_2 z}+e^{a_2(z+a_3(z+t-1))}}\right)H((z+t)-1)$$
$$+ \epsilon a_1 \left(e^{-\epsilon t}(\eta-\eta z)\right.$$
$$\left.+ \epsilon\left(\frac{1}{2a_3}e^{-\epsilon t}\left((z-1)^2\left(1+a_3\left(1+\eta(1+a_1(\epsilon t-1))\right)\right)\right)\right)\right) \tag{17}$$

$$c_v(z,t) = (\eta + \epsilon((1-\eta)t)H(1-(z+t)) \tag{18}$$
$$+ \left(\eta + \epsilon\left((1-\eta)t + \frac{1}{a_2 a_3}\ln\left(\frac{e^{a_2}}{e^{a_2}-e^{a_2 z}+e^{a_2(z+a_3(z+t-1))}}\right)\right)\right)H(z+t$$
$$-1) + \eta e^{-\epsilon t}$$
$$+ \epsilon\left(-e^{-\epsilon t}(-\eta a_1 + \eta a_1 z)\epsilon t + e^{-\epsilon t} + e^{-\epsilon t}\left(\left(\frac{1}{a_3}+1\right)(1-z)\right)\right)$$
$$- \left(\eta - \eta\epsilon t + \epsilon\left(\frac{1}{a_3}+1\right)(1-z)\right)$$

$$\psi_s(z,t) = \left(1 + \epsilon\left(\frac{a_1 a_3((\eta-1)e^{-a_2 t}(1+e^{a_2 t}((a_2 t-1))))}{a_2}\right)\right)H(1-(z+t)) \tag{19}$$
$$+ \left(\frac{e^{a_2}}{e^{a_2}-e^{a_2 z}+e^{a_2(z+a_3(z+t-1))}}\right)H((z+t)-1)$$

$$H(x) = \begin{cases} 1 & if\ x \geq 0 \\ 0 & if\ x \leq 0 \end{cases} \tag{20}$$

Results and Analysis

Figure 3 shows the particle distribution for the coffee particles ground by the Lelit PL53 (Espresso only grinder). The frequency volume distribution shows a bimodal distribution, where one peak is at around 50 µm and another peak is at around 500 µm. Figure

4 shows the particle size distribution of these sieved grains, where most of the particles in range of 300-600 μm was removed.
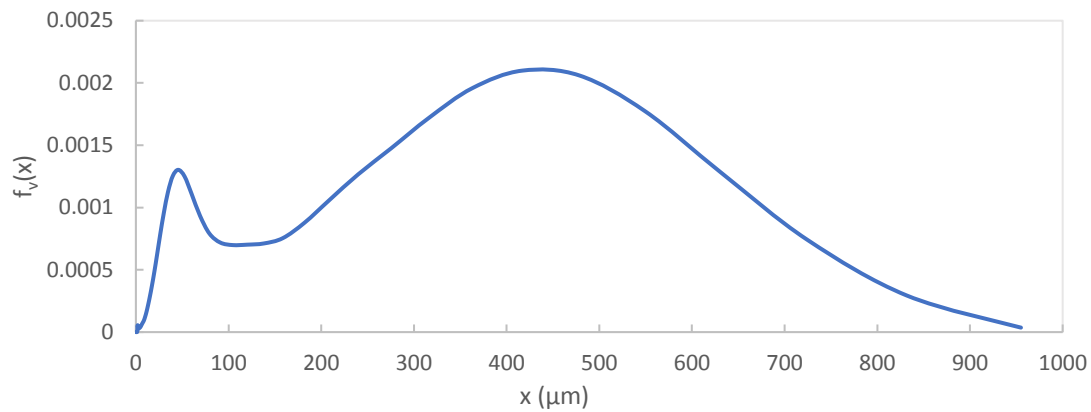

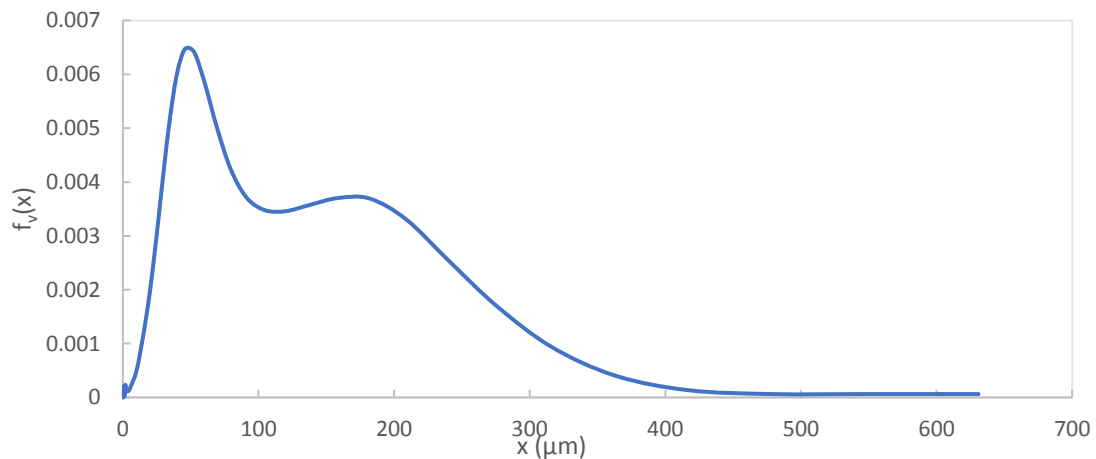*Figure 3 The frequency volume particle size distribution for normal grind size of Lelit PL53*

Figure 4 The frequency volume particle size distribution for coffee grinds after sieved through a 250 μm sieve

Figure 5 shows larger intact coffee cells and also smaller coffee cell fragments under the inverted microscope. Also, some representative particle sphericity was measured using the inverted microscope. The particles are not perfectly spherical, but for ease of further calculations, the particles were assumed to be spherical, meaning that their sphericity is 1.

Figure 6 shows that the large particles, seen as intact coffee cells, are porous in nature. Since the media composing the packed bed are also porous, when developing a mathematical model one can't simply rely on classical formulas such as Darcy's Law to explain the phenomena. A model should incorporate the double porosity nature in order to accurately show convection and diffusion through the media.
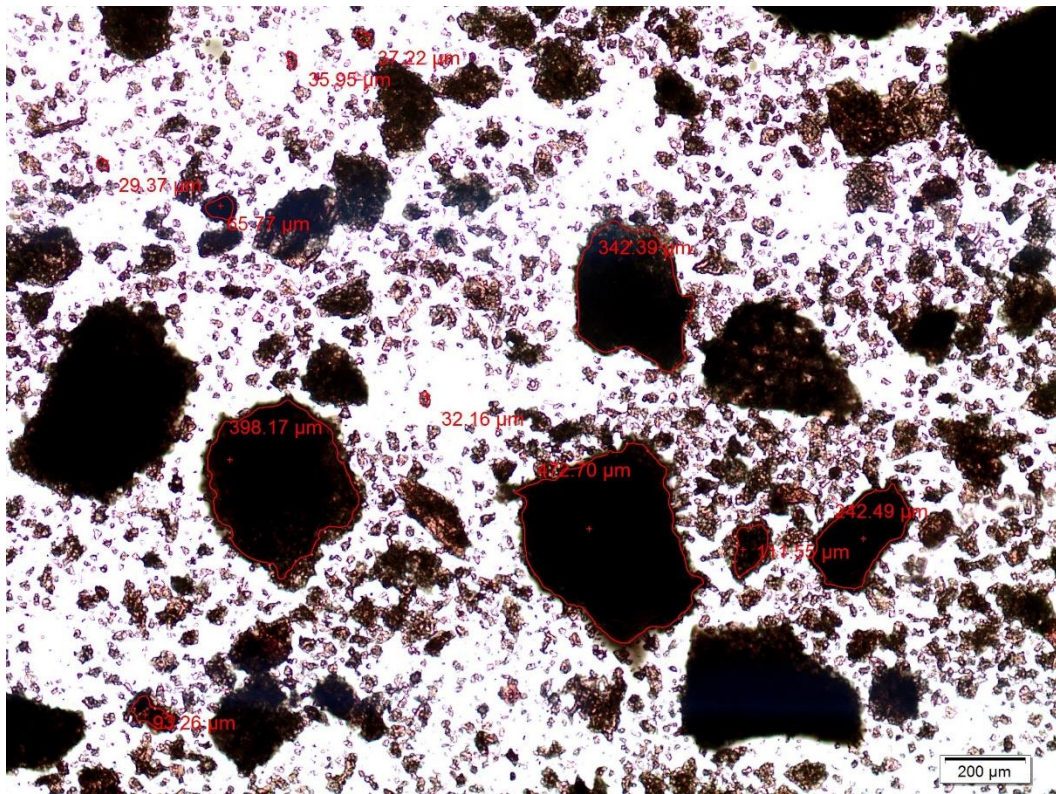
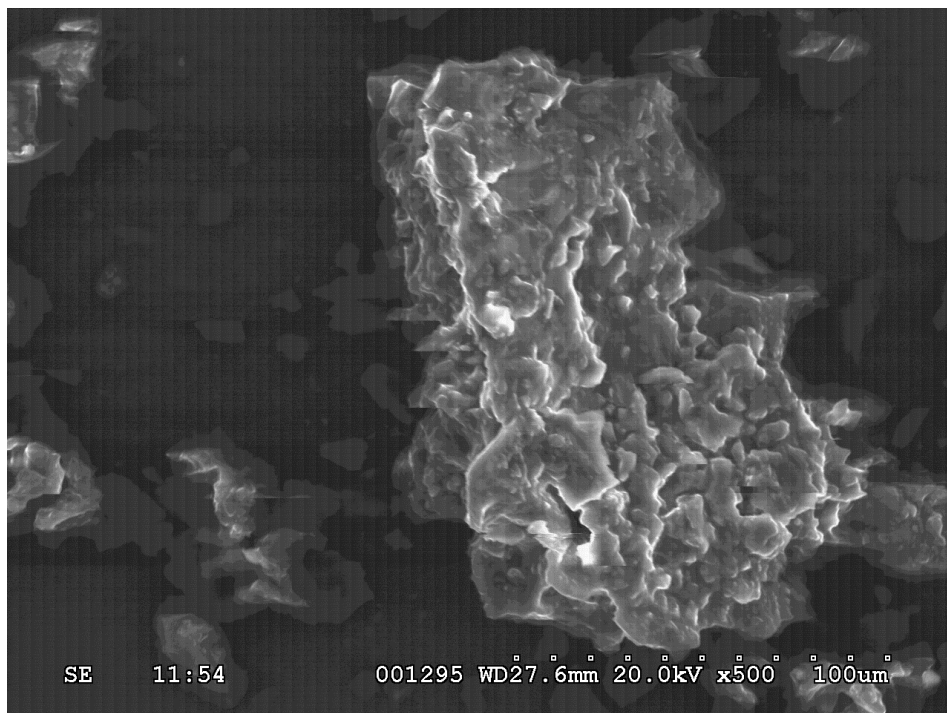*Figure 5 The coffee particle in the inverted microscope*

Figure 6 The intact coffee cell in the scanning electronic microscope showing its porous nature

It has been proposed that there are two distinct stages of coffee extraction. The initial extraction is fast, which can be explained by the reduced mass transfer resistance in the cell fragments. The mass diffusion in the pores inside the intact coffee cells may account for the following slow extraction. [5]

Figure 7 shows percent extraction as a function of the mass ratio for the 4 sets of trials. It shows that the 3 data sets that had the same grind size, behave similarly in extraction yield when the mass is nondimensionalized. The data seems to show that the smaller particles are able to achieve higher extraction percentages when compared to the data from the normal grind size at the same mass ratio. This is potentially because the mass is more concentrated on the surface of the small particles, while the larger intact coffee cells are more porous in nature. Since, the mass is more concentrated on the surface of the smaller particles, the mass transfer coefficient is larger than that of the of the intact coffee cells causing them to reach higher extraction percents. Figure 8 shows percent extraction with respect to the percentage of dissolved solids present in the espresso. Percentage of dissolved solids is often used to determine the strength of the coffee, or how concentrated the coffee is. Figure 6 shows that the smaller coffee particles tend to produce coffee with higher extraction percentages when compared to espresso of similar strengths.
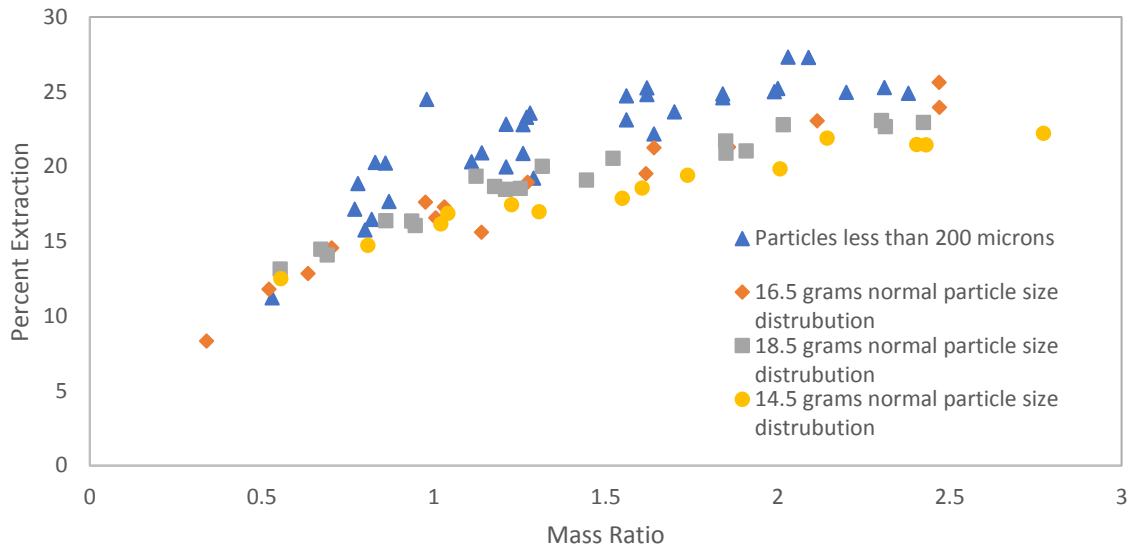
Figure 7 Extraction as a function of mass ratio with different mass in coffee bed and particle size distribution
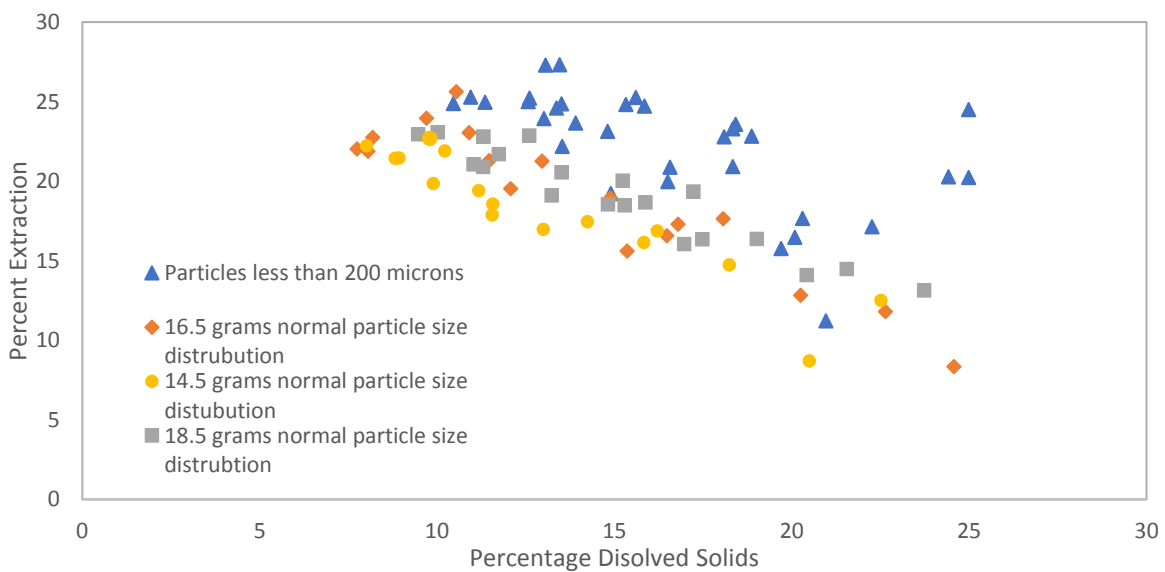

Figure 8 Extraction as a function of total dissolved solids with different mass in coffee bed and particle size distribution

After solving this system of partial differential equations we generated a figure of extraction percent with respect to the dimensionless time using the asymptotic solution to the concentration in h phase for espresso brewing. As we see in Figure 9, the extraction percent increases fast in the beginning of the plot. The potential reason to account for this phenomenon is that the compounds in coffee were extracted out fast initially. Also, we can see that the extraction percent approaches to 14.4% as the time increases, where the possible reason to explain this effect is that the coffee bed reaches its limit of soluble coffee and there's no more compounds can be extracted out. In Figure 10 we can see the extraction

percent calculated using our parameters. For our espresso, the extraction percent increase slower and reach a higher extraction in a longer time. The possible reason for the higher extraction to occur is that the grind size for our coffee is not identical to theirs, which results in the different dominant mechanism in the extraction process. Also, the pressure change from Moroney et al.[5] is 230000 Pa, but the pressure change in our espresso machine is 900000 Pa. Theoretically, the extraction percent should increase faster with our espresso machine. Figure 10 doesn't follow our expectations, which could be an evidence that the mathematical model does not fit to our data. Additionally, some concerns about mass conservation were noted.
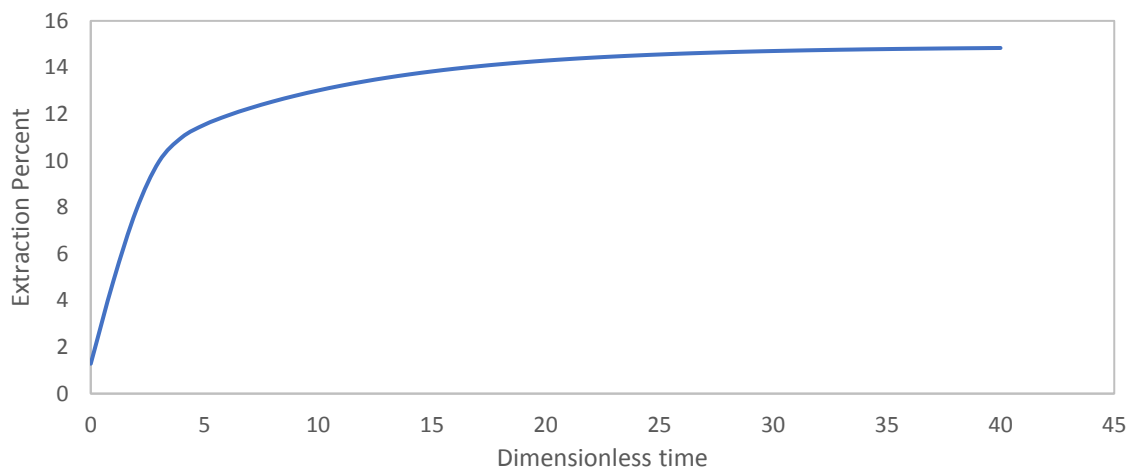
Figure 9 The extraction as a function of dimensionless time for values from Moroney et al[5]
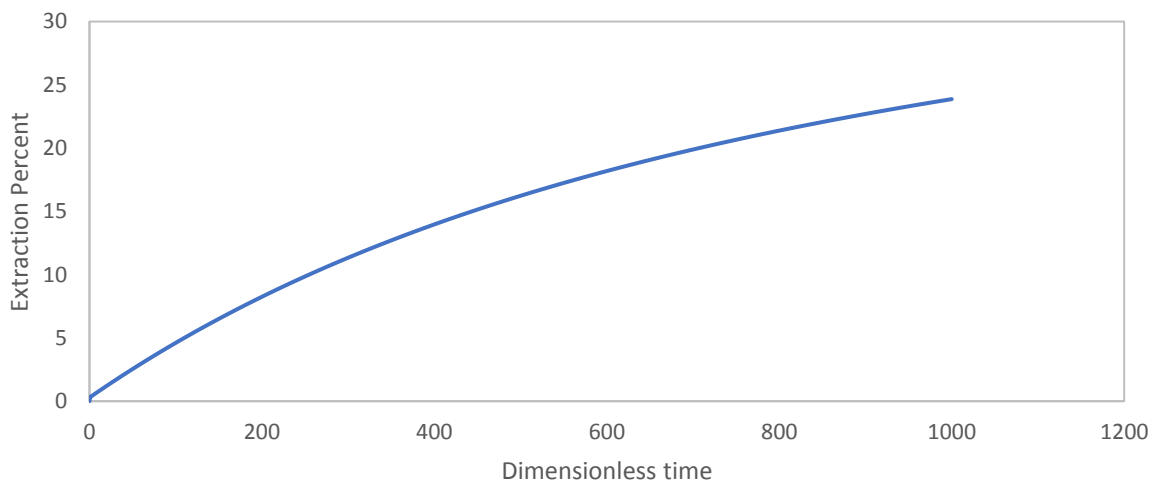

Figure 10 The extraction as a function of dimensionless time for our experimental values

The PDA, and mass spectrometry for the sieved, and normal grind size coffee can be found in Appendix C. After comparing the mass spectrum of each peak for both the sieved and the normal grind coffee, it was determined that the compounds extracted from them are mostly the same. Therefore, we draw a conclusion that the particle size is not a factor that will impact the composition of the espresso.

Conclusions and Future Work

Overall our research shows that small broken coffee cells are able to achieve higher extraction percentages when compared to coffee made using a mixture of intact coffee cells and broken coffee cells. This leads us to the conclusion that the smaller particles have a higher percentage of mass on their surface, leading to a larger mass transfer coefficient, while still producing a brewed coffee that is largely chemically identical.

In the future, we would like to further investigate, develop, and improve a better mathematical model, that better fits our experimental data. Other methods of coffee brewing besides espresso could also be investigated. Also we would like to work on determining how the composition of coffee changes during different points of the extraction.

References

[1]S. Topik, "Coffee as a Social Drug", *Project Muse*, 2017. .

[2]"An Intuitive Guide To Coffee Solubles, Extraction And TDS", *Handground.com*, 2017. [Online]. Available: https://handground.com/grind/an-intuitive-guide-to-coffee-solubles-extraction-and-tds. [Accessed: 16- Aug- 2017].

[3]C. Taira, "Improving Espresso - Getting Dialed", *meticulist*, 2017. [Online]. Available: http://www.meticulist.net/blog/improving-espresso-getting-dialed. [Accessed: 16- Aug- 2017].

[4]D. Shechter, "Pharmaceutical Size Reduction: How Size Affects Stability, Appearance & Properties", *Beei.com*, 2016. [Online]. Available: http://www.beei.com/blog/pharmaceutical-size-reduction-how-size-affects-stability-appearance-properties. [Accessed: 16- Aug- 2017].

[5]K. Moroney, W. Lee, S. O'Brien, F. Suijver and J. Marra, "Asymptotic Analysis of the Dominant Mechanisms in the Coffee Extraction Process | SIAM Journal on Applied Mathematics | Vol. 76, No. 6 | Society for Industrial and Applied Mathematics", *Epubs.siam.org*, 2016. [Online]. Available: http://epubs.siam.org/doi/abs/10.1137/15M1036658. [Accessed: 16- Aug- 2017].

[6]K. Moroney, W. Lee, S. O'Brien, F. Suijver and J. Marra, "Modelling of coffee extraction during brewing using multiscale methods: An experimentally validated model - ScienceDirect", *Sciencedirect.com*, 2015. [Online]. Available: http://www.sciencedirect.com/science/article/pii/S0009250915004108. [Accessed: 16- Aug- 2017].

Appendix A. Assumptions used in Asymptotic Analysis of the Dominant Mechanisms in the Coffee Extraction Process

1. It is assumed that the system is in isothermal conditions during brewing as the temperature variations are considered negligible.
2. It is assumed that all pores in the coffee bed are saturated with fluid.
3. It is assumed that the coffee bed properties are homogeneous in any cross-section based on the cylindrical geometry of the coffee bed and nature of the flow.
4. It is assumed that all coffee particles are spherical.
5. It is assumed that the concentration of the solid coffee matrix c_s is constant.
6. It is assumed that as coffee dissolves, the grain porosity changes rather than the solid concentration.
7. It is assumed that there is a coffee concentration c_{sat} which is the concentration in the liquid phase that would be in equilibrium with the concentration in the solid phase.
8. It is assumed that the diffusive flux is zero at the outlet.
9. It is assumed that only caffeine is extracted from the coffee.
10. It is assumed that the diffusion of the coffee is the rate limiting step.
11. It is assumed that the solid coffee in the cell walls within the grains dissolves into the intragranular pores very quickly initially so that all soluble coffee in the grains is dissolved in the fluid in the intragranular pores initially.
12. It is assumed that all the soluble coffee in the grain kernels has dissolved in the intragranular pores.
13. It is assumed that the initial concentration profile for the fine grind considered is at coffee solubility throughout the bed.
14. It is assumed that the initial concentration profile for coarser grind is a linear profile varying from 0 at the filter entrance to the initial exiting concentration c_{max} at the filter exit.
15. It is assumed that without modeling the initial water infiltration, uniformly decrease $\Psi_s^*(z^*,0)$ to correspond to the amount of coffee which has dissolved to give $c_h^*(z^*,0)$.

Appendix B. Maple Code used to numerically solve the equations presented in Asymptotic Analysis of the Dominant Mechanisms in the Coffee Extraction Process

Maple numeric integration of Moroney et al.[5] SIAM J. Appl. Math., 76, 2196-2217 (2016).

Solving the nondimensionalized equations (2.27) - (2.29) with boundary conditions (2.31) - (2.32)

First set up the constants. These are the values used in their work and are used to check our solution against their.

$$eps := 3.03 \cdot 10^{-2} :$$

$$a1 := 2.81 :$$

$$a2 := 0.0149 :$$

$$a3 := 0.473 :$$

$$eta := 0.5 :$$

$$psiSZero := 0.7304 :$$

$$DeltaP := -900000 :$$

$$L := 0.011 :$$

$$PhiS := 1 :$$

$$mu := 3.15 \cdot 10^{-4} :$$

$$m := 1.76 \cdot 10^{-4} :$$

$$phiH := 0.2 :$$

PDE1 represents (2.27) and is the solution to Ch, which is the concentration of coffee in the h phase. Here, h represents

the space between grains of coffee (intergranular phase)

$$PDE1 := eps \cdot \frac{\partial}{\partial t} cH(z, t) = \frac{\partial}{\partial z} cH(z, t) - eps \cdot a1 \cdot cH(z, t) + cV(z, t) + (1 - a1 \cdot eps \cdot cH(z, t)) \cdot psiS(z, t)$$

PDE2 represents (2.28) and is the solution to Cv, which is the concentration of coffee in the v phase. Here, v represents

the porous space inside the grains (intragranular phase)

$$PDE2 := \frac{\partial}{\partial t} cV(z, t) = a1 \cdot eps \cdot cH(z, t) - cV(z, t)$$

PDE3 represents (2.29) and is the solution to capital psi in S. The s phase is the coffee solid phase, which should dissolve away through the extraction process.

Lower case psi represents the fraction of coffee remaining in the phase. The main assumption here is that the s phase has coffee at the surface and in the kernels, but only

the surface contributes due to the short duration of espresso extraction. Capital psi, which (2.29) solves, is a nondimensional version of psi.

$$PDE3 := eps \cdot \frac{\partial}{\partial t} psiS(z, t) = -1 \cdot a2 \cdot a3 \cdot (1 - a1 \cdot eps \cdot cH(z, t)) \cdot psiS(z, t)$$

$$PDEs := \{PDE1, PDE2, PDE3\}$$

Initial and boundary conditions:

$$IBCs := \left\{ cH(z, 0) = \frac{1}{(a1 \cdot eps)}, cV(z, 0) = eta, psiS(z, 0) = \frac{a2 \cdot psiSZero}{(a1 \cdot eps)}, cH(1, t) = 0 \right\}$$

Solve it numerically

$$pds := pdsolve(PDEs, IBCs, numeric, time = t, 'spacestep' = 0.0005, range = 0..1)$$

Trying a plot of cV to match Figure 7

$$plots[display]\left(\left[seq\left(pds{:}{-}plot\left(cV, t = \frac{i}{eps} \right), i = 0..10 \right)\right]\right)$$

Trying a plot of cV to match Figure 9

$$plots[display]\left(\left[seq\left(pds{:}{-}plot\left(\frac{psiS \cdot a1 \cdot eps}{a2 \cdot psiSZero}, t = \frac{i}{10} \right), i = 0..10 \right)\right]\right)$$

$$p1 := pds{:}{-}plot(cV, t = 0, numpoints = 50) :$$
$$p2 := pds{:}{-}plot(cV, t = 2 \cdot eps, numpoints = 50, color = blue) :$$
$$p3 := pds{:}{-}plot(cV, t = 6 \cdot eps, numpoints = 50, color = green) :$$

$p1 := pds:-plot(psiS, t = 0, numpoints = 50):$
$p2 := pds:-plot(psiS, t = 1 \cdot eps, numpoints = 50, color = blue):$
$p3 := pds:-plot(psiS, t = 6 \cdot eps, numpoints = 50, color = green):$

$$pds:-animate\left(\frac{psiS \cdot a1 \cdot eps}{a2 \cdot psiSZero}, t = 0.75, frames = 150, title = \text{"time} = \%f\text{"}\right)$$

$$pds:-animate(cH \cdot a1 \cdot eps, t = 0.75, frames = 150, title = \text{"time} = \%f\text{"})$$

$$pds:-animate(cV, t = 0.75, frames = 150, title = \text{"time} = \%f\text{"})$$

$$vS := \frac{\dfrac{DeltaP}{L}}{-\dfrac{150 \cdot mu}{PhiS^2 \cdot m^2} \cdot \dfrac{(1 - phiH)^2}{phiH^3}}$$

$$Q := vS \cdot Pi \cdot \left(\frac{58.3 \cdot 10^{-3}}{2}\right)^2$$

$$pds:-animate\left(\frac{cH \cdot Q \cdot a1 \cdot eps}{0.0165}, t = 0.75, frames = 150, title = \text{"time} = \%f\text{"}\right)$$

Appendix C. The PDA and mass spectrometry results for both sieved and normal grind size coffee.
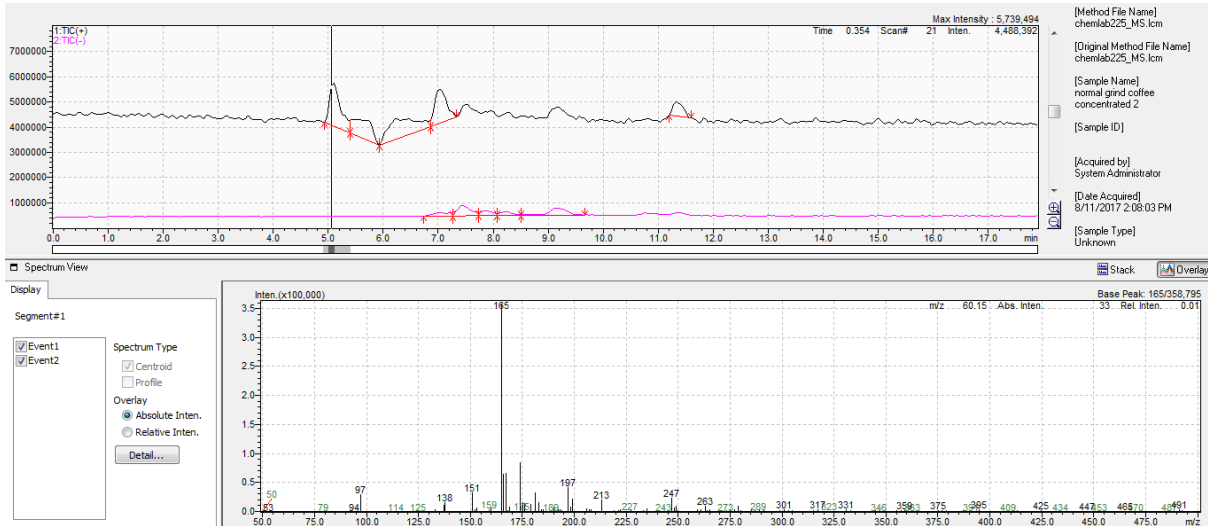
Figure 11 Peak 1 of mass spectrometry for espresso brewed with normal grind size coffee
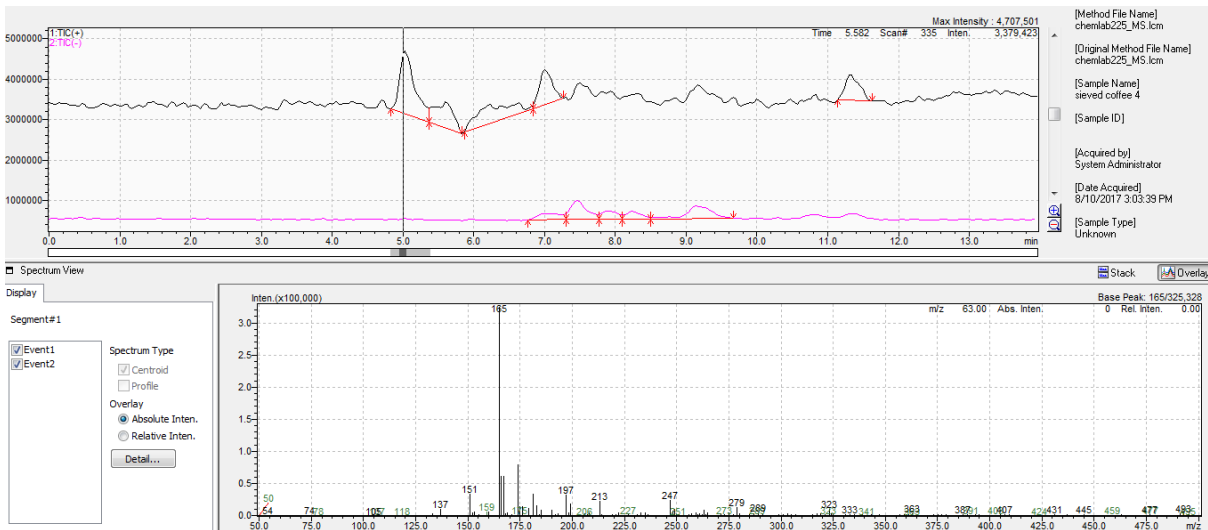
Figure 12 Peak 1 of mass spectrometry for espresso brewed with sieved coffee
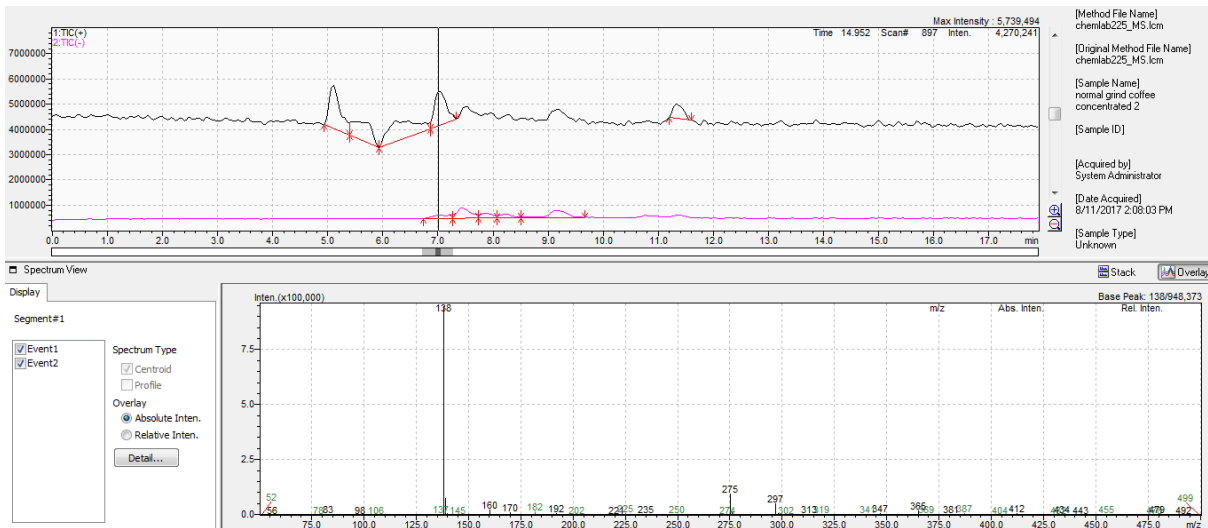
Figure 13 Peak 2 of mass spectrometry for espresso brewed with normal grind size coffee
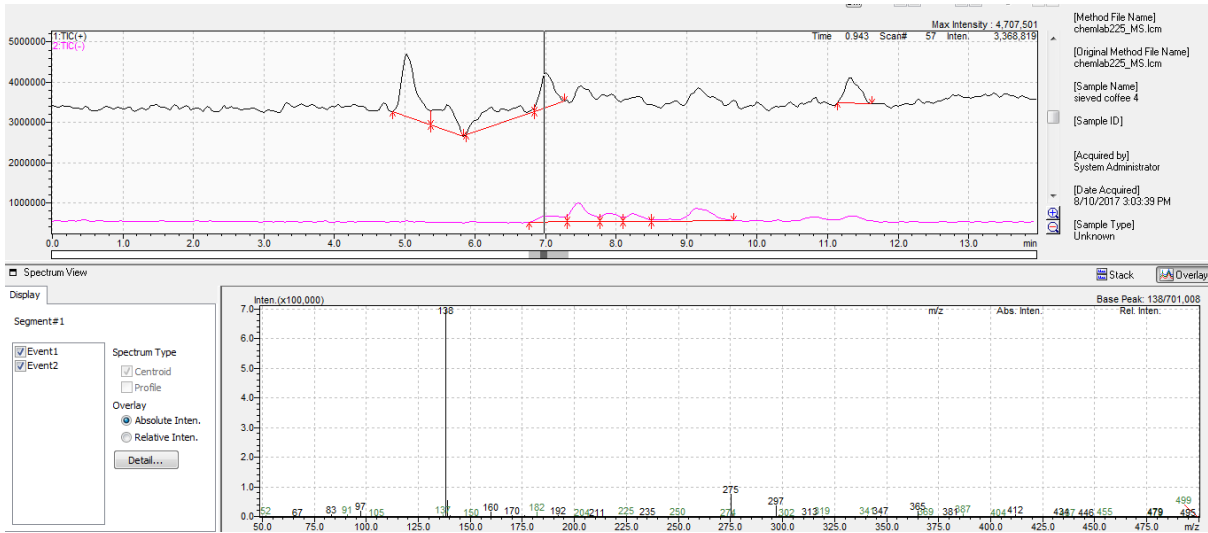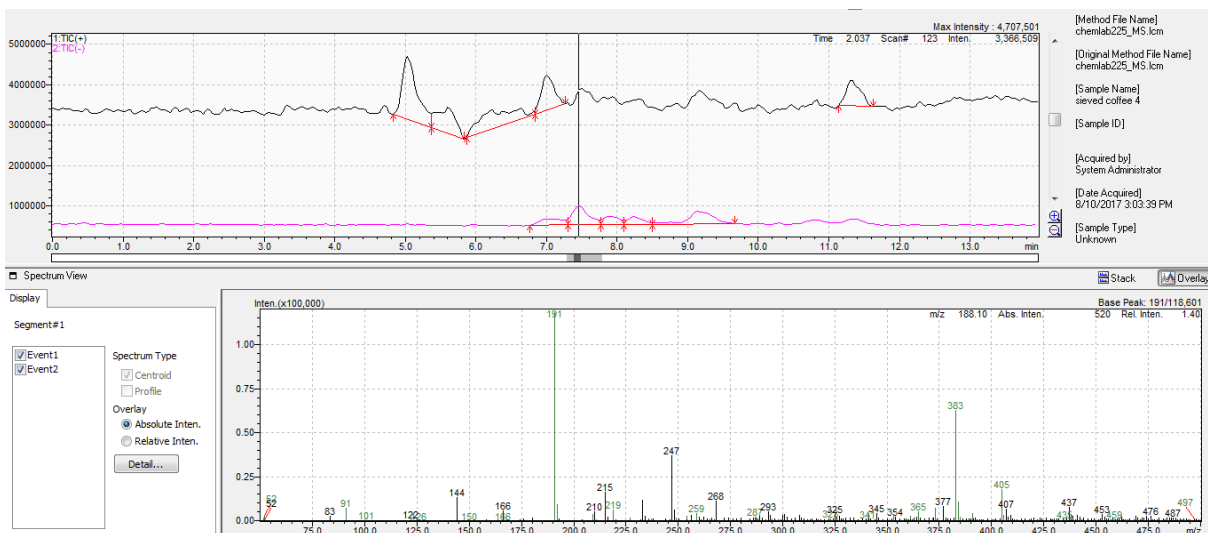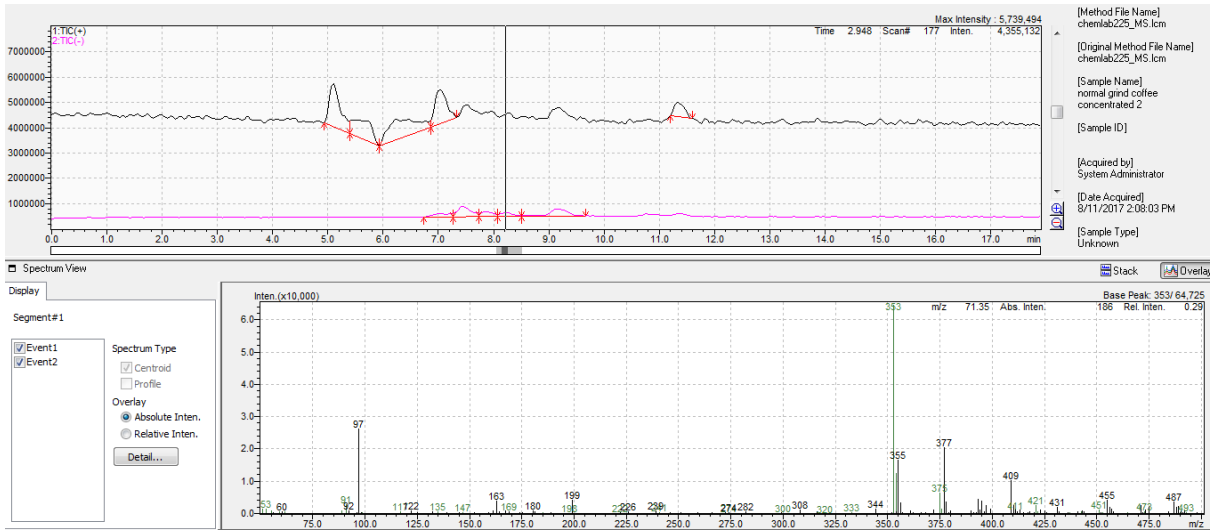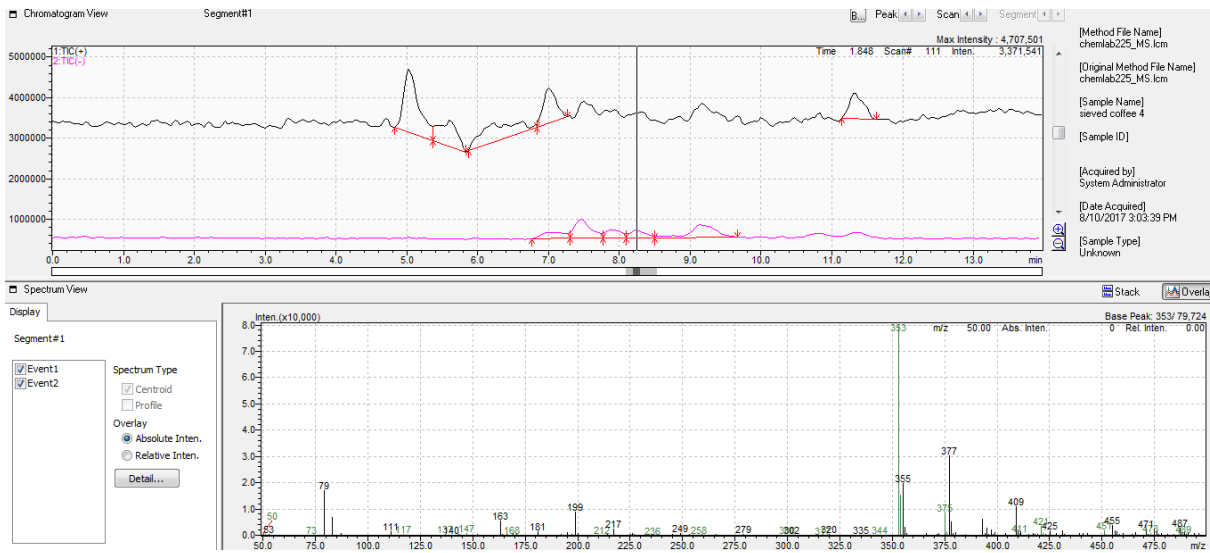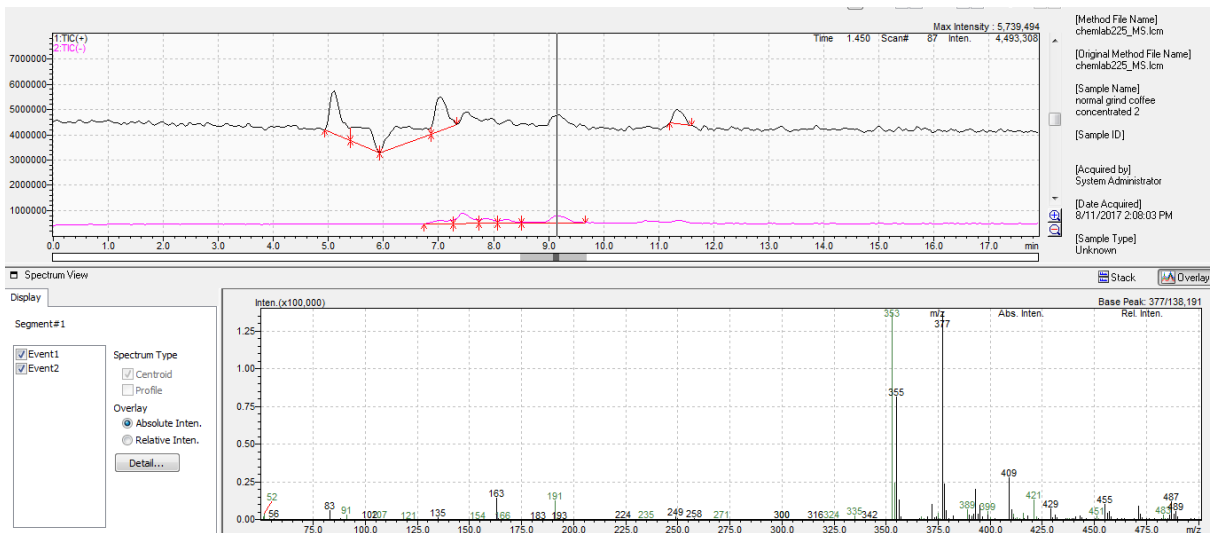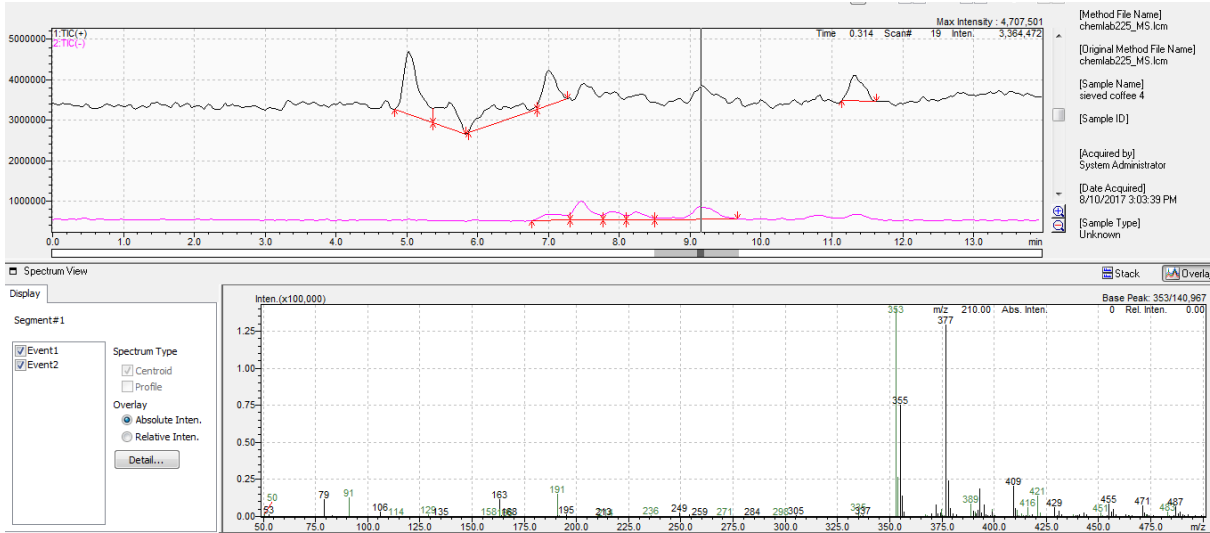
Figure 14 Peak 2 of mass spectrometry for espresso brewed with sieved coffee
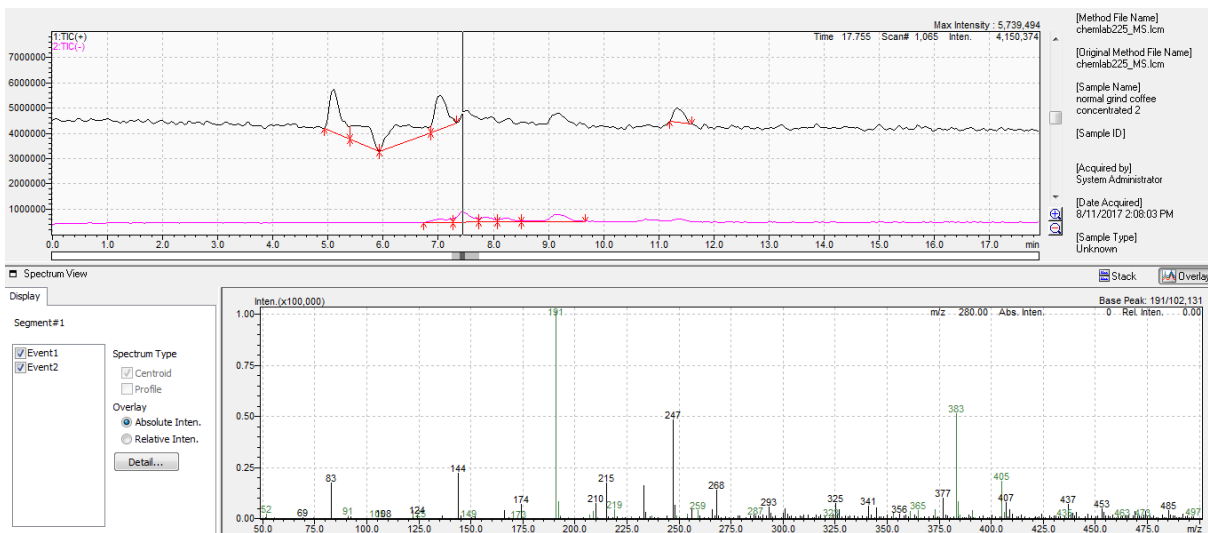
Figure 15 Peak 3 of mass spectrometry for espresso brewed with normal grind size coffee

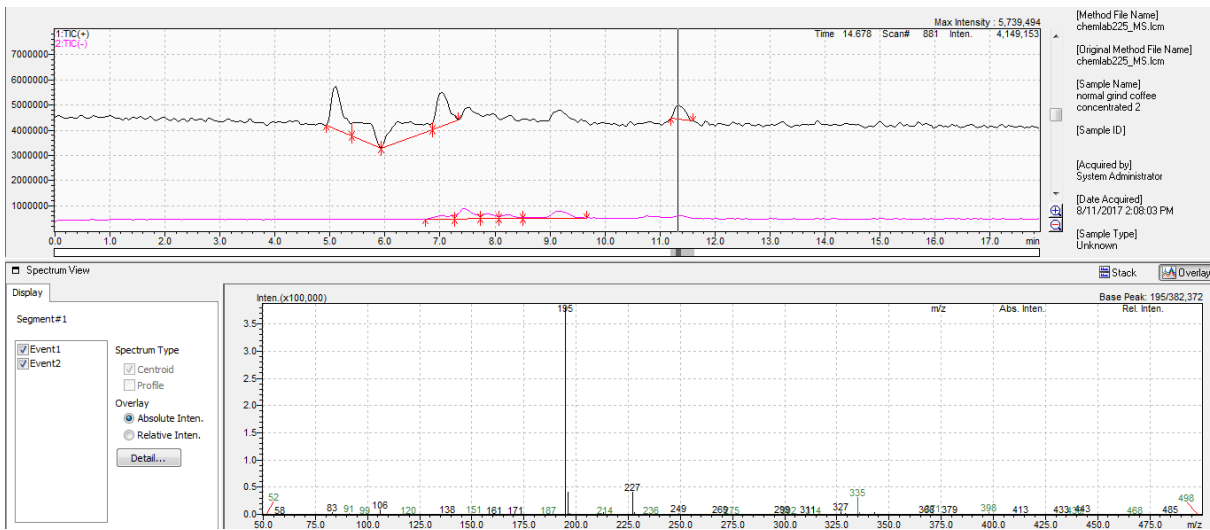*Figure 16 Peak 3 of mass spectrometry for espresso brewed with sieved coffee*

Figure 17 Peak 4 of mass spectrometry for espresso brewed with normal grind size coffee

Figure 18 Peak 4 of mass spectrometry for espresso brewed with sieved coffee

Figure 19 Peak 5 of mass spectrometry for espresso brewed with normal grind size coffee

Figure 20 Peak 5 of mass spectrometry for espresso brewed with sieved coffee

Figure 21 Peak 6 of mass spectrometry for espresso brewed with normal grind size coffee
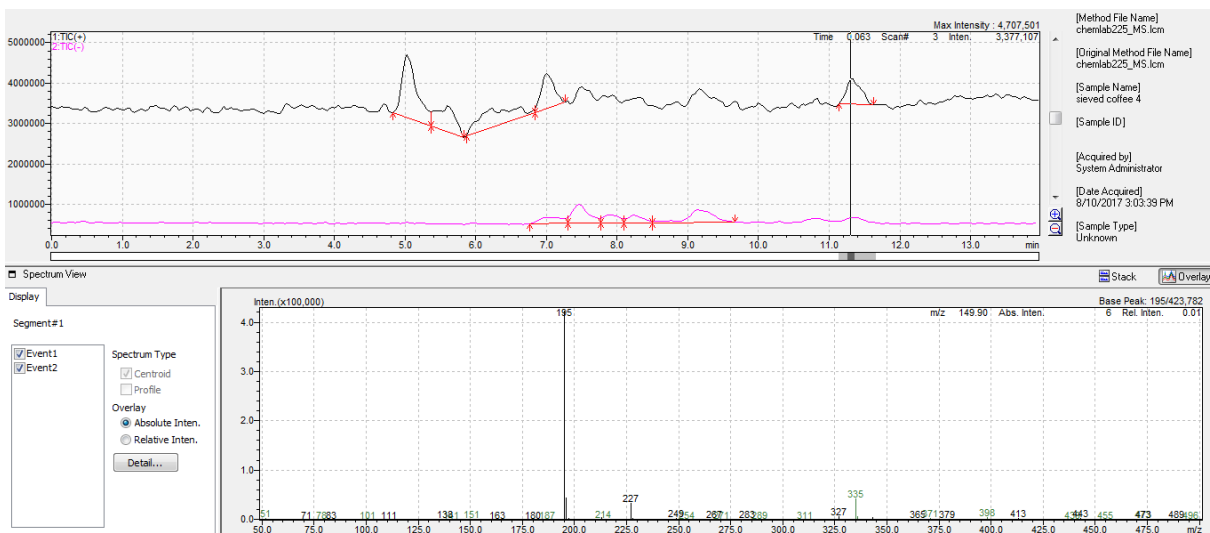

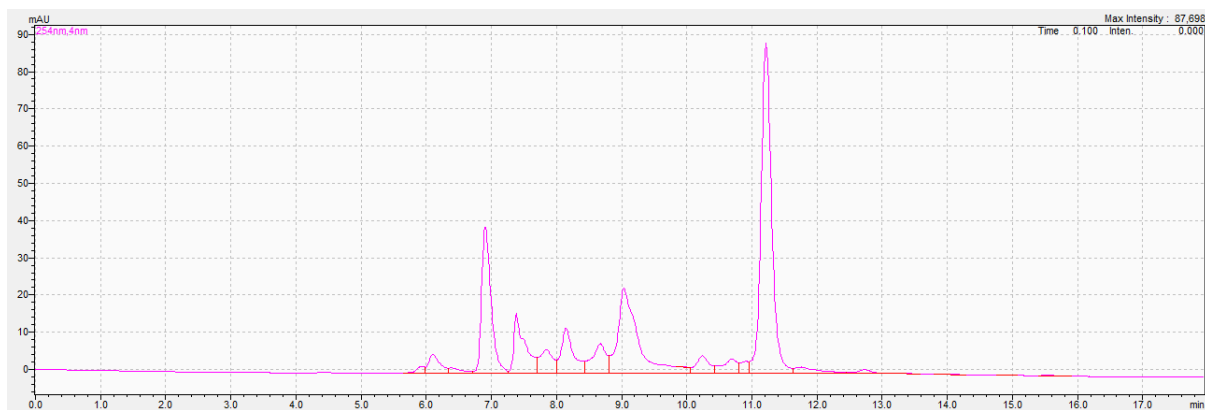*Figure 22 Peak 6 of mass spectrometry for espresso brewed with sieved coffee*

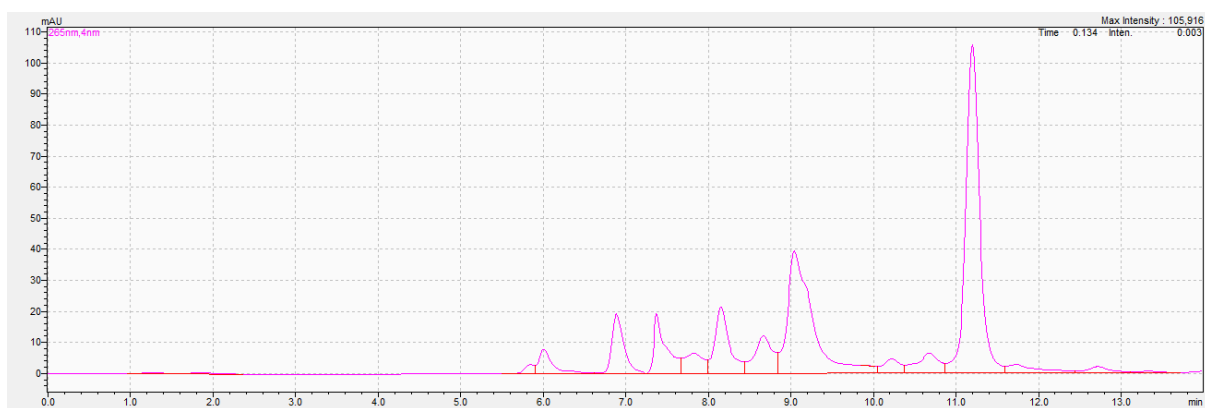*Figure 23 PDA at 265 nm for espresso brewed with normal grind size coffee*

Figure 24 PDA at 265 nm for espresso brewed with sieved coffee